

# Real-time feedback controlled monomer conversion: a new paradigm for UV curing process control

*Thomas Hafkamp<sup>1</sup>, Gregor van Baars<sup>2</sup>, Bram de Jager<sup>1</sup>, Pascal Etman<sup>1</sup>*

*<sup>1</sup>Dept. of Mechanical Engineering, Eindhoven University of Technology, Eindhoven, The Netherlands*

*<sup>2</sup>Dept. of Equipment for Additive Manufacturing, TNO, Eindhoven, The Netherlands*

## Abstract

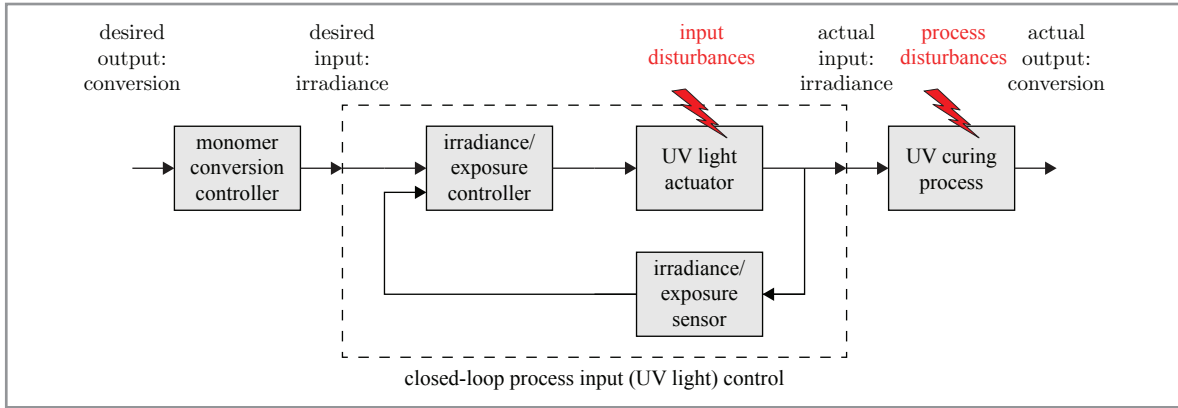
Process monitoring and control systems are typically limited to supervision of exposure conditions in the UV curing industry. Although it is generally desirable to measure and control process inputs and boundary conditions such as exposure, superior performance can be expected from a system that controls the actual process output in closed loop. Following this line of reasoning in the context of 3D printing, the present work proposes to measure and control the degree of monomer conversion online and in closed loop in order to reject disturbances. To this end, a spectrometer was used to acquire in-situ measurement data, compare the data with the desired process trajectory using a real-time feedback controller, and compute a corrective action for the UV light source. The experimental results demonstrate that the closed-loop controller was successful in rejecting a purposely applied input disturbance, while the open-loop controller was unsuccessful in meeting the final cure level target. These promising first results prove the principle and might give rise to a new paradigm in UV curing process control.

## Introduction

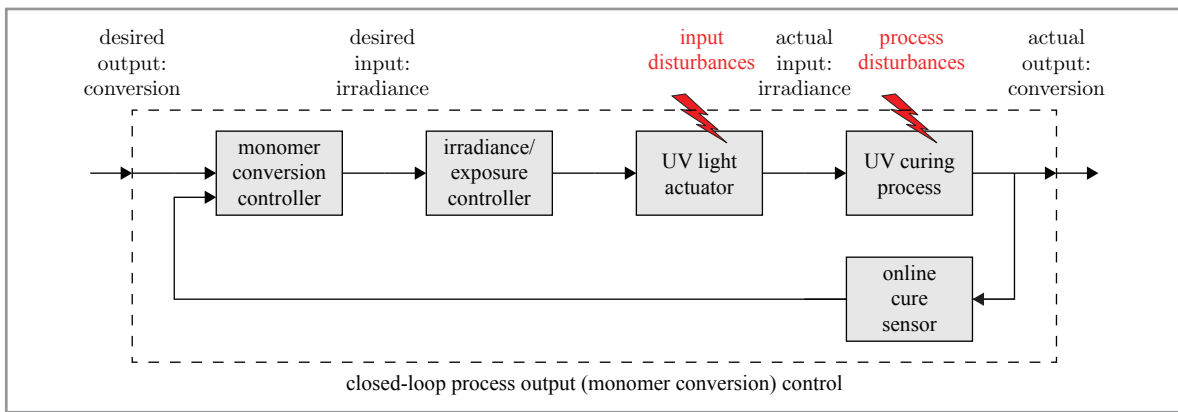
Process monitoring and control systems<sup>1</sup> are indispensable tools for quality management in manufacturing processes in general,<sup>2</sup> and for polymerization reactions<sup>3,4</sup> such as UV curing<sup>5</sup> specifically. Process control schemes with closed feedback loops contribute to a reduced sensitivity to disturbances and model uncertainties,<sup>1,2</sup> which ultimately leads to improved production yield, productivity and consistency in end-product quality.

Although a vast body of literature is available on UV cure monitoring,<sup>3,6,7</sup> only few works<sup>4,8–10</sup> report on efforts to control the UV curing process *output* in closed loop. The reason may be that a cost-effective or simple online sensor of the extent of cure is still not readily available. Instead, UV curing process monitoring and control systems typically rely on feedback of radiometric measurements of the *input* irradiance or exposure conditions at the surface,<sup>5,11</sup> as visualized in Figure 1 (a). In the latter control configuration, the achievable disturbance rejection performance is limited in comparison to the former control configuration where the actual process output (conversion) is included in the feedback loop,<sup>2</sup> as visualized in Figure 1 (b). The best performance may be achieved in a situation where both are controlled in closed-loop, for instance in the cascaded configuration shown in Figure 1 (c).

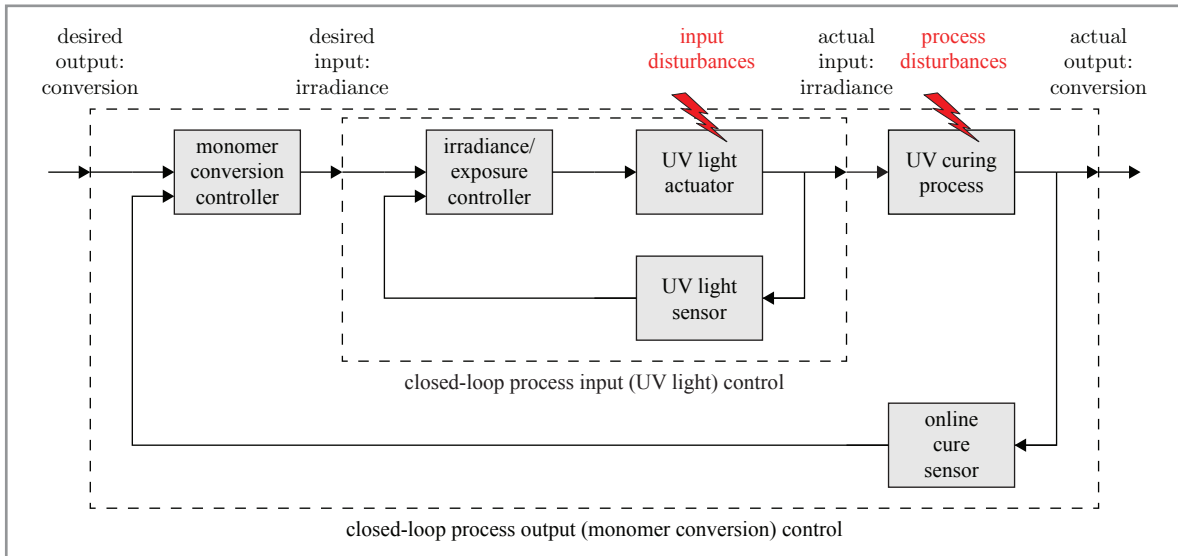
To the best of the author's knowledge, no reports exist of attempts to control the degree of monomer conversion in closed loop in the context of UV curing. Despite the fact that the cure extent is not easily



(a) closed-loop UV curing *process input* control



(b) closed-loop UV curing *process output* control



(c) cascade of closed-loop *process input* & closed-loop *process output* control

**Figure 1:** Comparison of UV curing control schemes where the *process input* is controlled (a) versus where the *process output* is controlled (b) versus where they are *both* controlled (c) in closed loop.

measured,<sup>5</sup> the potential benefits of using closed-loop control can be explored in a research lab environment, irrespective of the specific sensing technology and related system integration challenges faced by UV curing equipment manufacturers. Recent work by the present authors reflects on these challenges in the context of photopolymer-based additive manufacturing (AM).<sup>7,12</sup> The need for advancing the measurement science for these polymer-based AM processes is widely recognized by the industry.<sup>13</sup>

This paper presents, complementary to our recent findings,<sup>12</sup> an experimental proof of principle of real-time feedback control for UV curing processes in which the degree of monomer conversion is the controlled variable. This proof is given by comparing degree of conversion outputs in situations with and without feedback control and under disturbed conditions. Contrary to our previous work,<sup>12</sup> an artificial input disturbance is applied to create these disturbed conditions to mimic real-world disturbances. Rejecting said disturbances is the objective of feedback control, where the final aim is to make the UV curing process more robust and increase end-product quality.

## Methods

UV curing processes inherently have a spatial dependence due to the absorption of UV light with propagation depth into the layer.<sup>14</sup> However, the UV curing process can be considered homogeneous if one draws the system boundary on a sufficiently small scale. This homogeneous situation allows to demonstrate what could be achieved with a feedback controller if one had full control over the UV light's spatial distribution. Furthermore, this situation allows to consider the UV curing process as a simple single-input-single-output (SISO) system, whose only input and output are UV light intensity and degree of monomer conversion respectively, as illustrated in Figure 2.

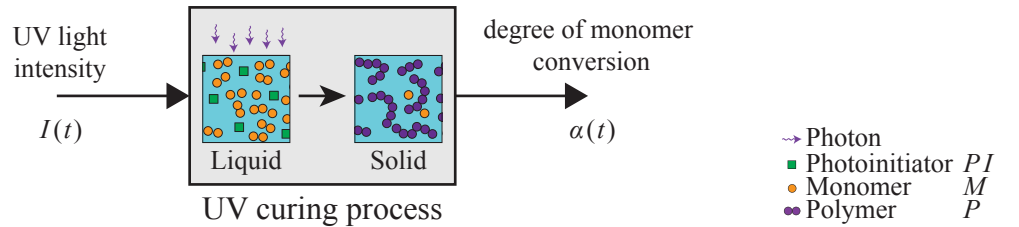


**Figure 2:** Single-input-single-output system view of the UV curing process.

## FTIR spectroscopy equipment

The desired homogenous situation was approximated by depositing a thin photopolymer layer and only measuring a small portion at the bottom of layer. To this end, a Fourier-transform infrared (FTIR) spectrometer (Thermo Scientific Nicolet 6700) was used in attenuated total reflection (ATR) mode (Smart Orbit ATR accessory). The FTIR spectrometer was expanded with a 405 nm UV LED (Bivar UV5TZ-405-30) to control the light intensity and an embedded controller (Raspberry Pi 3 Model B) to compute the control actions. These control actions were computed by a control scheme that was first implemented in the MATLAB/Simulink environment on a Master PC and then deployed to the embedded controller. To enable the use of the FTIR spectrometer as an online sensor, custom software was developed for real-time communication of measurement data. Figure 3 shows an overview of the complete embedded control system used in this study.

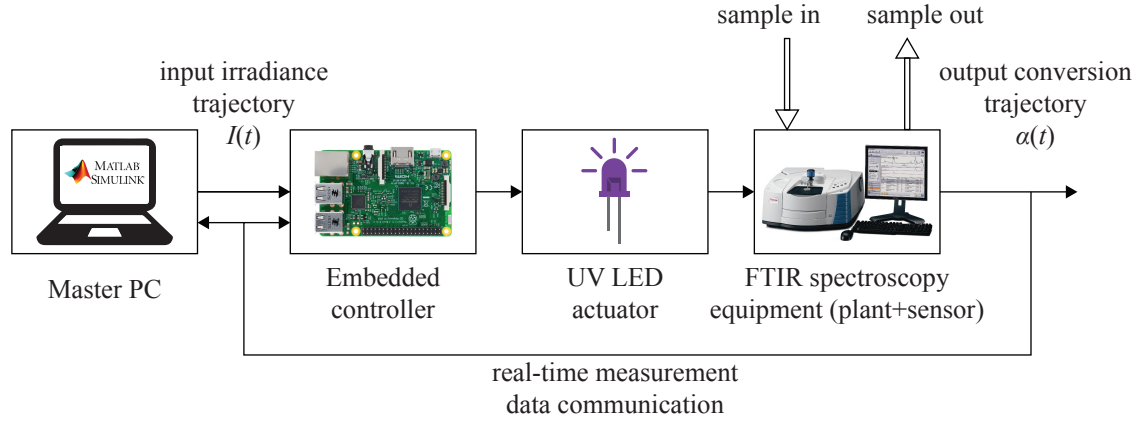


**Figure 3:** Block diagram of the embedded control system for real-time UV curing process control. An interfacing master PC deploys a control scheme onto an embedded controller, which in turn actuates a UV LED's light intensity. The UV LED illuminates a thin photopolymer layer in an FTIR spectrometer, whose conversion is measured at the bottom and communicated in real-time to the embedded controller. Image adapted from.<sup>12</sup>

Using this system, IR absorbance spectra were obtained in the wavenumber region 400 to 4000  $\text{cm}^{-1}$  at a sampling rate of one spectrum per  $T_s = 2.0$  s. The degree of conversion  $\alpha_m(t)$  was obtained from the baseline-corrected peak area ratio<sup>15</sup> of the C=C peak at 1635  $\text{cm}^{-1}$  and the aromatic reference peak at 1608  $\text{cm}^{-1}$ .

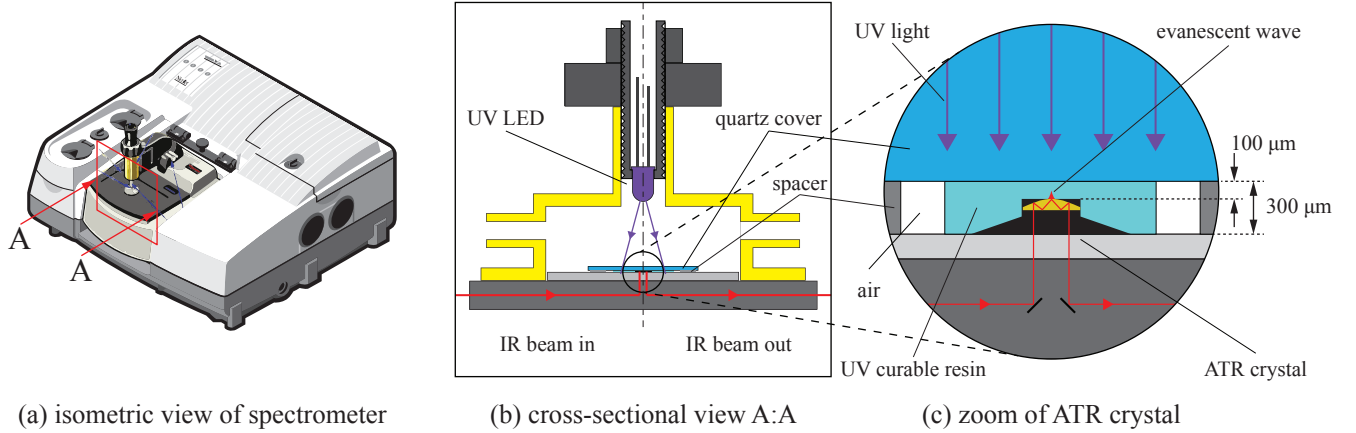
### Photopolymer sample preparation

Figure 4 schematically shows a cross-section of the UV LED and the sample on the ATR accessory mounted on the FTIR spectrometer. The UV LED is mounted in a cup that is placed above the center of the ATR crystal. For each sample, a droplet of material was deposited onto the ATR crystal, a 300  $\mu\text{m}$  thick steel spacer was placed around it, and a 1 mm thick quartz window (Thorlabs) was placed on top. The resulting layer thickness above the ATR crystal was approximately 100  $\mu\text{m}$  due to the 200  $\mu\text{m}$  protrusion height of the crystal, see Figure 4. To better match the conditions during 3D printing, the experiments were purposely performed without flushing with nitrogen on forehand and carried out at 20 °C room temperature. Without loss of generality, an acrylate-based 3D printing resin for dental applications (NextDent SG) was used in this work (NextDent, Soesterberg, The Netherlands).

### Experimental procedure

Three types of experiments were carried out and compared to demonstrate the benefits of using a closed-loop conversion controller:

1. open-loop parameter identification experiments under nominal (non-disturbed) conditions;
2. open-loop control experiments under disturbed conditions;
3. closed-loop control experiments under disturbed conditions.



**Figure 4:** Schematic overview of the spectrometer, ATR crystal, and sample. Image adapted from.<sup>12</sup>

Figure 5 shows a block scheme of each experiment type. During the open-loop experiments, the UV light source was simply turned on and off using a feedforward intensity  $I_{FF}(t)$ . An artificial input disturbance  $v(t)$  was applied to show the functionality of the feedback controller. Alternative ways to apply a disturbance were previously explored.<sup>12</sup> The input disturbance consisted of a negative bias at half the intensity level of the feedforward intensity:  $v(t) = -0.5 \cdot I_{FF}(t)$ . Thus, the effective UV light intensity is halved in the disturbed case. This case mimics the situation where the UV light source has severely deteriorated to a point where it only delivers 50 % of its original irradiance. Instead of digitally applying this disturbance, one could also insert a physical optical filter into the light path.

Firstly, the open-loop parameter identification experiments were carried out without the input disturbance to parameterize a simple process model. The samples were irradiated for 90 s at an irradiance level of  $3.8 \text{ W/m}^2$ . A feedforward input trajectory  $I_{FF}(t)$  and a reference trajectory  $\alpha_{ref}(t)$  were then generated from this process model. The objective for the closed-loop or feedback controller was to track this reference trajectory even under disturbed conditions. Secondly, the open-loop control experiments were performed *without* a feedback controller but with the input disturbance to show its effect on the output. Finally, the closed-loop control experiments were conducted *with* a feedback controller and with the input disturbance to demonstrate the workings of the controller. Both the open-loop and the closed-loop control experiments were performed with a feedforward intensity of  $3.8 \text{ W/m}^2$  and irradiation time of 60 s.

### UV curing process model

A simple process model was developed to approximate the behaviour of the UV light-initiated photopolymerization reaction.<sup>12</sup> The differential equation describing the monomer concentration is:

$$\frac{d[M](t)}{dt} = -cI^b(t)[M]^n(t) \quad (1)$$

$$\alpha(t) = 1 - \frac{[M](t)}{[M]_0}, \quad (2)$$

where  $[M]$  is the monomer concentration,  $c$  is a constant representative for the reaction rate,  $I$  is the irradiance,  $b$  is a constant between 0.5 and 1,<sup>16</sup>  $n$  is the reaction order,  $\alpha$  is the degree of conversion, and

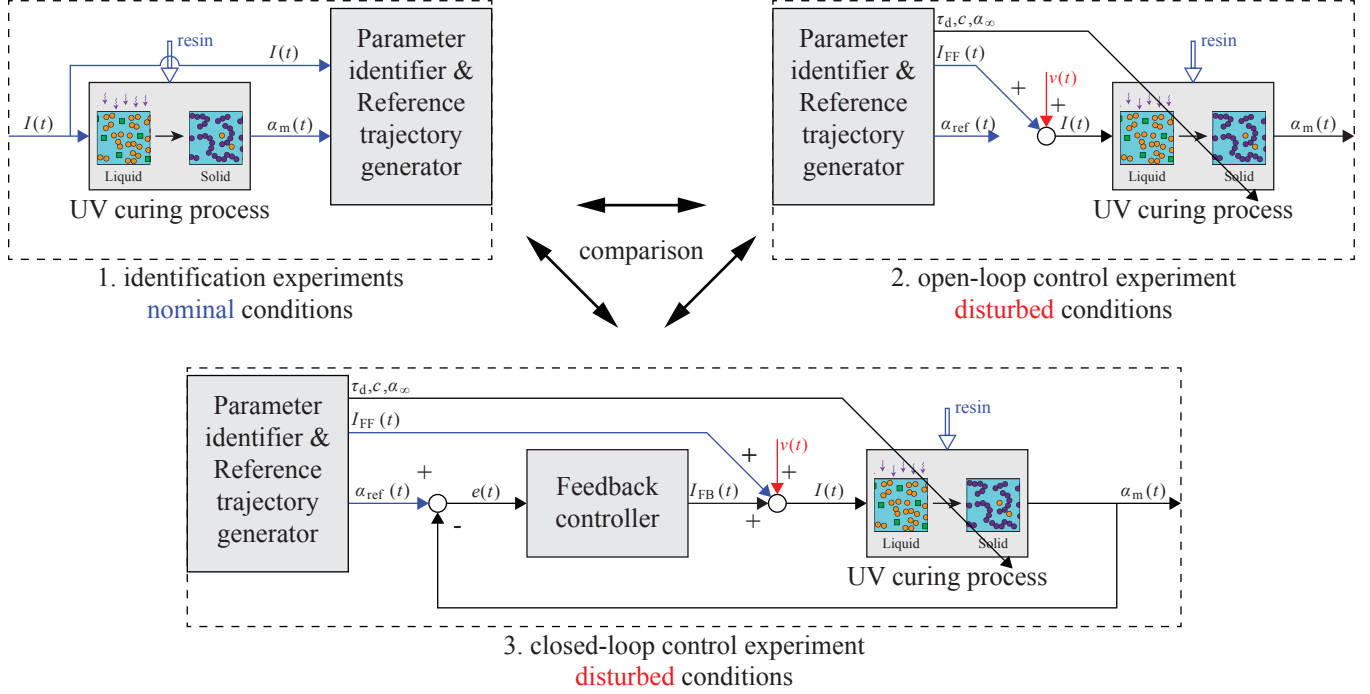


**Figure 5:** Block schemes of the parameter identification, open-, and closed-loop control experiments. Nominal (non-disturbed) conditions are indicated in blue and disturbed conditions are indicated in red. Image adapted from.<sup>12</sup>

$[M]_0$  is the initial monomer concentration.

To complete the model, the initial condition is added that  $[M](0) = [M]_0$  and the physical constraint is imposed that both irradiance and monomer concentration are non-negative  $I(t) \geq 0, [M](t) \geq 0$ . Moreover, a scale factor  $\alpha_\infty$  is introduced to model the asymptotic behaviour that the monomer conversion never reaches 100 % in practice:

$$\alpha_m(t) = \alpha_\infty \alpha(t), \quad (3)$$

where  $\alpha_m(t)$  is the modelled or measured absolute degree of conversion.

The differential model (1) has an explicit solution<sup>12</sup> when subjected to a constant or step input irradiance  $I(t)$ , which facilitates the parameter identification process. The following step input was applied in the simulation model:

$$I_{FF,d}(t) = \begin{cases} 0, & t < t_{step} + \tau_d \\ I_{step}, & t_{step} + \tau_d \leq t < t_{end} \\ 0, & t \geq t_{end}. \end{cases} \quad (4)$$

where  $t_{step}$  is the time when the light turns on,  $\tau_d$  is a time delay, and  $t_{end}$  is the time the light turns off. The time delay  $\tau_d$  was used to model the initiation period in the free-radical photopolymerization reaction.<sup>12</sup> This time delay  $\tau_d$  was only applied in the simulations to generate the reference trajectory  $\alpha_{ref}(t)$  from the model (1); the time delay was not applied during physical experiments.

## Controller design

The proportional-integral-derivative (PID) controller is widely used in industrial process control<sup>17</sup> and thus was used in this study. The derivative action was omitted to prevent aggressive reactions to noise in the output signal and an integrator reset was incorporated to reduce integral windup. The resulting proportional-integral (PI) controller typically has the form:<sup>1,17</sup>

$$I_{FB}(t) = K_c \left[ e(t) + \frac{1}{\tau_I} \int_0^t e(t) dt \right], \quad (5)$$

where  $I_{FB}$  is the corrective action,  $K_c$  is the *proportional* gain,  $\tau_I$  the *integral* time, and the error signal  $e(t) = \alpha_{ref}(t) - \alpha_m(t)$ . The total light intensity  $I(t)$  requested from the UV LED actuator is the sum of the feedforward and the feedback intensities  $I(t) = I_{FF}(t) + I_{FB}(t)$ , as depicted in the third situation in Figure 5.

## Results

### Parameter identification experiments

The parameter identification experiments were carried out ten times under the same nominal conditions, so without the input disturbance. Figure 6 shows the resulting degree of conversion as a function of time for a single experiment. The analytical solution of model (1) was fitted to the experimental data through least-squares parameter estimation in MATLAB. The exponent  $b$  was set to 0.5 to use the well-known square-root dependency<sup>14</sup> between the reaction rate and the light intensity, which was verified in a separate set of experiments.<sup>12</sup> The reaction order  $n$  was set to one and two respectively and Figure 6 shows that the latter yields a better fit to the experimental data. Figure 7 shows scatter and box plots to indicate the uncertainty of the identified model parameters and Table 1 gives the final parameters.

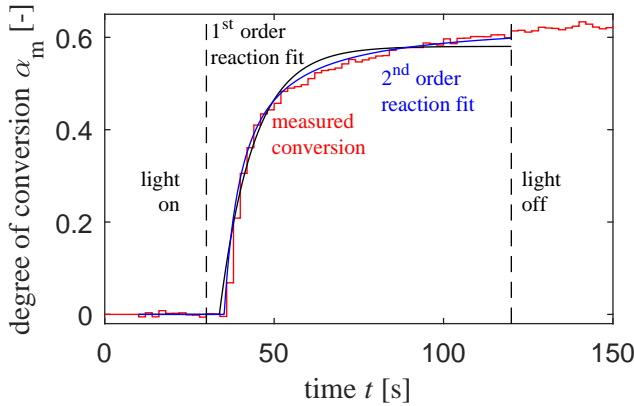


**Figure 6:** Degree of conversion obtained from FTIR measurements, and first- and second-order reaction model fits.

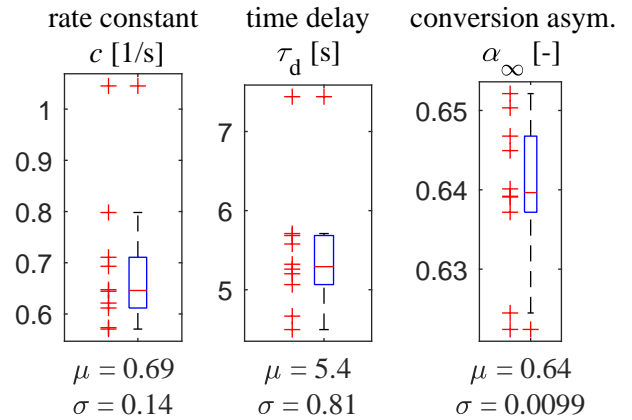


**Figure 7:** Scatter and box plots of identified model parameters based on ten replications of the parameter identification experiment.

Resin	$b$ [-]	$n$ [-]	$c$ [ $s^{-1}$ ]	$\tau_d$ [s]	$\alpha_\infty$ [-]	$K_c$ [-]	$\tau_I$ [s]
NextDent SG	0.5	2	$0.69 \pm 0.14$	$5.4 \pm 0.8$	$0.64 \pm 0.01$	4	80

**Table 1:** The identified model parameter means  $\pm$  standard deviations and tuned controller parameters.

### Open- and closed-loop control experiments

The open- and closed-loop experiments were carried out with an input disturbance. Subsequently, the PI controller parameters  $K_c$ ,  $\tau_I$  were determined by manually tuning on the physical system. Figures 8 and 9 show the resulting degree of conversion output and normalized input respectively for the three cases to be compared: the nominal non-disturbed case, the open-loop disturbed case, and the closed-loop disturbed case.

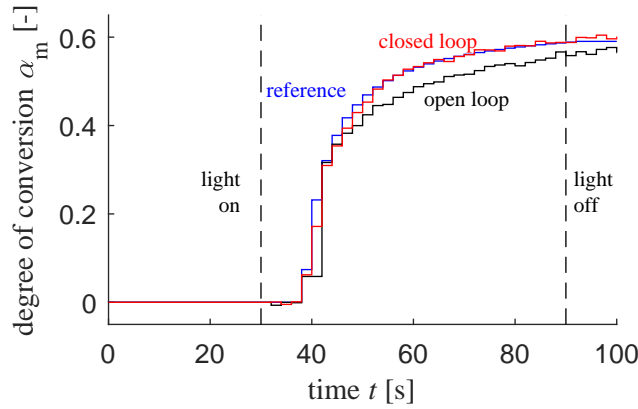


**Figure 8:** Degree of conversion output for the nominal non-disturbed, open-loop disturbed, and closed-loop disturbed case.

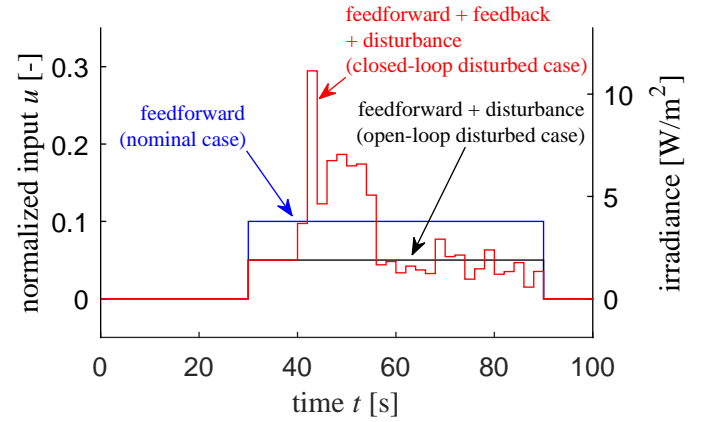


**Figure 9:** Total irradiance input for the nominal non-disturbed, open-loop disturbed, and closed-loop disturbed case.

The results in Figure 8 clearly exemplify the effect of the input disturbance on the open-loop case, i.e., the reaction speed decreases with respect to the nominal case. As a result, the final conversion level does not meet the target at the end of the exposure time. However, the closed-loop results show that the feedback controller successfully compensates for the input disturbance by requesting more power from the UV LED, as observed in Figure 9. Therefore, the working principle of a real-time feedback controller has been experimentally demonstrated for a UV curing process.

### Discussion

The present work mainly demonstrates that a feedback controller can successfully reject input disturbances to the UV curing process. This main result, together with a similar result previously obtained for physical process disturbances to the feedstock material,<sup>12</sup> provides a proof of principle for closed-loop control of the primary UV curing process output. Referring back to the control system configuration in Figure 1 (b), both an *input disturbance* and a *process disturbance* respectively were intentionally applied to perturb the UV curing process. Indeed, one could argue that the input disturbance case could also be handled by the closed-loop process input controller in Figure 1 (a). However, a major advantage is that



the closed-loop process output control strategy in Figure 1 (b) can handle both types and other types of disturbances that appear inside the loop.

Certainly, one of the main reasons to reject disturbances is to improve the end-product quality.<sup>2</sup> The question is, however, whether meeting the cure level target at the end of the exposure time is sufficient to assure product quality metrics such as material properties. The implications of not meeting the conversion target may be detrimental to mechanical properties in UV curing applications. So it seems reasonable that the closed-loop case outperforms the open-loop case in Figure 8, since the former meets the final conversion target while the latter does not. However, the material properties may be a function of the complete time evolution of conversion. This function may be similar to the nonreciprocity relationship between the irradiance level (exposure power), exposure time, and exposure dose.<sup>11,18</sup> Nevertheless, the monomer conversion control loop could be an essential element of a larger cascaded control scheme like the one in Figure 1 (c), where the conversion is an input to a sequential material property build-up process.<sup>19</sup>

Various limitations of the present work need to be overcome before the proposed control approach can be implemented into UV curing manufacturing processes. A discussion on such implementation aspects in large-scale photopolymer-based AM machines was previously presented.<sup>12</sup> In any case, a degree of conversion sensor needs to be developed that meets the requirements of the specific UV curing process. Relevant aspects include the temporal resolution or sampling rate in relation to the polymerization reaction timescale,<sup>18</sup> the spatial resolution or size of the volume that is measured, the probe design and its sampling configuration,<sup>20</sup> and the stationarity or mobility of the photocurable resin with respect to sensors and actuators.

## Conclusion

The present work proposes to measure and control the degree of conversion in real time and in closed loop to reduce the sensitivity to disturbances. To study this proposition, an FTIR spectrometer was integrated into a real-time control system with a UV LED actuator and a feedback controller. An artificial input disturbance was applied and the open-loop controlled case was compared to the closed-loop controlled case. The closed-loop control results showed improved conversion tracking performance in comparison to the open-loop results and hence proves the principle of feedback control for input disturbance rejection in UV curing processes. Although various implementation challenges remain, such closed-loop control schemes may prove an indispensable tool in the UV curing industry's ever-increasing need for improved yield, productivity and end-product quality.

## Acknowledgements

This study was funded by the Netherlands Organisation for Applied Scientific Research (TNO) and was carried out within the AMSYSTEMS Center. The authors would like to thank their colleagues from the TNO Materials Sciences department for their support and use of FTIR spectrometry equipment.

## References

- [1] B. A. Ogunnaike and W. H. Ray, *Process dynamics, modeling, and control*. Topics in chemical engineering, New York: Oxford University Press, 1994.

- [2] D. Hardt, "Modeling and control of manufacturing processes: Getting more involved," *Journal of Dynamic Systems, Measurement, and Control*, vol. 115, pp. 291–300, June 1993.
- [3] W. F. Reed and A. M. Alb, eds., *Monitoring polymerization reactions: from fundamentals to applications*. Hoboken, New Jersey: John Wiley & Sons, Inc, 2014.
- [4] T. Scherzer, K. Heymann, G. Mirschel, and M. R. Buchmeiser, "Process Control in Ultraviolet Curing with in-line near Infrared Reflection Spectroscopy," *Journal of Near Infrared Spectroscopy*, vol. 16, pp. 165–171, June 2008.
- [5] R. Schwalm, *UV coatings basics, recent developments and new applications*. Amsterdam; London: Elsevier, 1st ed., 2006.
- [6] G. E. Fonseca, M. A. Dubé, and A. Penlidis, "A Critical Overview of Sensors for Monitoring Polymerizations," *Macromolecular Reaction Engineering*, vol. 3, pp. 327–373, Sept. 2009.
- [7] T. Hafkamp, G. van Baars, B. de Jager, and P. Etman, "A feasibility study on process monitoring and control in vat photopolymerization of ceramics," *Mechatronics*, vol. 56, pp. 220–241, Dec. 2018.
- [8] F. Zeng, *Estimation and Control of Robotic Radiation-Based Processes*. PhD thesis, Clemson University, Clemson, SC, 2010.
- [9] A. M. Yebi, *Model-based control of UV curing processes with application to additive manufacturing*. PhD thesis, Clemson University, Clemson, SC, 2015.
- [10] X. Zhao, *Process Measurement and Control for Exposure Controlled Projection Lithography*. PhD thesis, Georgia Institute of Technology, Atlanta, GA, 2017.
- [11] R. W. Stowe, "Non-Reciprocity of Exposure of UV-Curable Materials and the Implications for System Design," in *RadTech 2016 UV & EB Technical Conference Proceedings*, (Chicago, Illinois), 2016.
- [12] T. Hafkamp, G. van Baars, B. de Jager, and P. Etman, "Real-time feedback controlled conversion in vat photopolymerization of ceramics: A proof of principle," *Additive Manufacturing*, vol. 30, p. 100775, 2019.
- [13] J. Pellegrino, T. Makila, S. McQueen, and E. Taylor, "Measurement science roadmap for polymer-based additive manufacturing," Tech. Rep. NIST AMS 100-5, National Institute of Standards and Technology, Gaithersburg, MD, Dec. 2016.
- [14] G. G. Odian, *Principles of polymerization*. Hoboken, N.J: Wiley-Interscience, 4th ed., 2004.
- [15] J. Stansbury and S. Dickens, "Determination of double bond conversion in dental resins by near infrared spectroscopy," *Dental Materials*, vol. 17, pp. 71–79, Jan. 2001.
- [16] P. J. Bartolo, ed., *Stereolithography*. New York, NY: Springer US, 1st ed., 2011.
- [17] W. S. Levine, *Control system fundamentals*. Boca Raton, FL: CRC press, 2nd ed., 2011.
- [18] C. I. Fiedler-Higgins, L. M. Cox, F. W. DelRio, and J. P. Killgore, "Monitoring Fast, Voxel-Scale Cure Kinetics via Sample-Coupled-Resonance Photorheology," *Small Methods*, vol. 3, no. 2, p. 1800275, 2019.
- [19] K. H. J. Classens, "Multiphysical Modeling and Control of Photopolymerization for Additive Manufacturing," Master's thesis, Eindhoven University of Technology, Eindhoven, 2019.
- [20] J. L. Koenig, *Spectroscopy of polymers*. New York, NY: Elsevier, 1st ed., 1999.